Quantum theory of the cold-atom micromaser including gravity

Thierry Bastin* and John Martin†
Institut de Physique Nucléaire, Atomique et de Spectroscopie, Université de Liège au Sart Tilman, Bât. B15, B-4000 Liège, Belgium
(Received 1 December 2004; published 22 November 2005)

The quantum theory of the cold-atom micromaser including the effects of gravity is considered. We show that gravity does not break the special properties of the induced emission probability for the micromaser in the cold atom regime and rather new effects are predicted. In particular, we show that the cavity acts in the gravity field as an additional repulsive and attractive potential, resulting in quasibound states of the atomic motion. This feature gives rise to fine resonances in the induced emission probability that are not restricted to any particular cavity mode function, in contrast to the usual cold-atom micromaser. It is also shown that the atom is able to emit a photon inside the cavity, though classically it does not reach the interaction region. Predictions about the photon number statistics when the cavity is pumped by a flux of excited atoms are finally given. Unusual highly nonclassical "dragon" distributions are still predicted in the vertical geometry.

DOI: 10.1103/PhysRevA.72.053815 PACS number(s): 42.50.Pq, 42.50.Vk, 32.80.Lg

I. INTRODUCTION

The coupling of atomic motion and radiation fields is a central topic in quantum optics. In this last decade, the microwave amplification via z-motion-induced emission of radiation, referred to as the *mazer* action [1–4], has opened a new chapter of micromaser physics. In this process, cold atoms are sent unidirectionally through a microwave high-Q cavity (Fig. 1) and a new type of induced emission inside the cavity occurs when quantum effects of the atomic motion dominate. A summary of the studies devoted to this subject may be found in [5]. In all these previous papers, gravity effects on the quantized atomic motion are not considered. However, it has often been argued that the achievement of the cold atom micromaser regime would be a formidable experimental task as the atoms in this regime move so slowly that they start exactly to be extremely sensitive to earth gravity and are expected to fall down before entering or leaving the cavity region, breaking the unidirectionality of the atomic trajectories. Gravity action on particles of small velocities is currently observed in matter wave experiments [6]. Recently, Nesvizhevsky *et al.* [7,8] identified the lowest stationary quantum state of neutrons in the earth's gravitational field by measuring the neutron transmission between a horizontal mirror on the bottom and an absorber or scatterer on top.

A possible way to circumvent the gravity problem for the mazer action (avoiding working in a reduced gravity environment) so as to preserve the unidirectionality of the atomic trajectories is to consider a vertical geometry where the atoms are sent vertically in the direction of the cavity, similarly to cavity QED experiments reported in [9–16]. This paper is devoted to establish the quantum theory of the mazer action in this context, taking into account gravity effects on the vertical quantized atomic motion. We show that gravity does not break the special properties of the induced emission probability in the cold atom regime and we predict rather new effects related to this geometry. The connected problem of atoms interacting with travelling waves in the gravitation field was treated recently [17,18].

The paper is organized as follows. In Sec. II, the Hamiltonian modeling the vertical micromaser is presented. The wave functions of the system are described. The properties of the induced emission probability are then presented in Sec. III. The connection with the classical hot atom regime is discussed. The photon statistics of the vertical micromaser pumped by a flux of vertical launched atoms is described in Sec. IV. A brief summary of our results is finally given in Sec. V.

II. MODEL

A. The Hamiltonian

We consider a two-level atom moving in the gravity field along the vertical z direction on the way to a cavity which we define to be located in the range $0<z<L$ (see Fig. 2). No transverse motion is considered. The atom is coupled resonantly to a single mode ω of the quantized field present in the cavity. The atomic center-of-mass motion is described quantum mechanically and the usual rotating-wave approximation is made. In the interaction picture, the Hamiltonian reads

$$H=\frac{p^2}{2m}+m\mathcal{G}z+\hbar g u(z)(a^\dagger\sigma+a\sigma^\dagger), \tag{1}$$

where p is the atomic center-of-mass momentum along the z axis, m is the atomic mass, $\mathcal{G}$ is the acceleration due to gravity, $\sigma=|b\rangle\langle a|$ ($|a\rangle$ and $|b\rangle$ are, respectively, the upper and lower levels of the two-level atom), a and $a^\dagger$ are, respec-

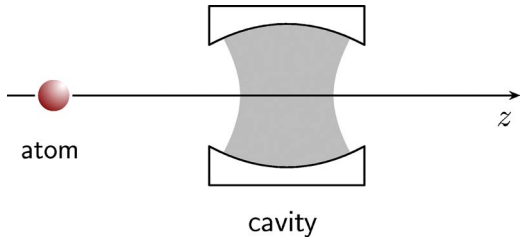

FIG. 1. (Color online) Scheme of the horizontal micromaser.

*Electronic address: T.Bastin@ulg.ac.be
†Electronic address: John.Martin@ulg.ac.be

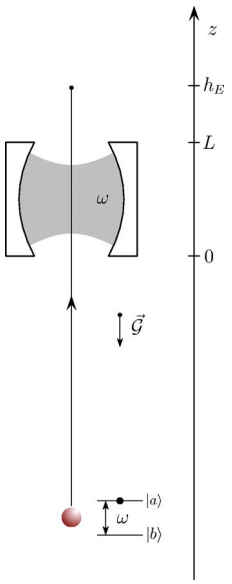

FIG. 2. (Color online) Scheme of the vertical micromaser.

tively, the annihilation and creation operators of the cavity radiation field, g is the atom-field coupling strength, and $u(z)$ is the cavity field mode function. We denote in the following the cavity field eigenstates by $|n\rangle$, the global state of the atom-field system at any time t by $|\psi(t)\rangle$, and the classical height attained by an atom of energy E in the gravity field by

$$h_E \equiv \frac{E}{m\mathcal{G}}. \tag{2}$$

B. The wave functions

In the z representation and in the dressed state basis

$$|\gamma_n^{\pm}\rangle = \frac{1}{\sqrt{2}}(|a,n\rangle \pm |b,n+1\rangle), \tag{3}$$

the global wave function components

$$\psi_n^{\pm}(z,t) = \langle z, \gamma_n^{\pm}|\psi(t)\rangle \tag{4}$$

obey the time-dependent Schrödinger equation

$$i\hbar\frac{\partial}{\partial t}\psi_n^{\pm}(z,t) = \left[-\frac{\hbar^2}{2m}\frac{\partial^2}{\partial z^2} + m\mathcal{G}z + V_n^{\pm}(z)\right]\psi_n^{\pm}(z,t) \tag{5}$$

with

$$V_n^{\pm}(z) = \pm\hbar g\sqrt{n+1}\,u(z). \tag{6}$$

Each $\psi_n^{\pm}(z,t)$ component encounters the potential $V_n^{\pm}(z)$ subject to the external linear gravitational potential $m\mathcal{G}z$ (see Fig. 3). The atom-field interaction reduces to a scattering problem in the presence of the gravitational field.

The general solution of Eq. (5) reads

$$\psi_n^{\pm}(z,t) = \int_{-\infty}^{\infty} c_n^{\pm}(E)e^{-iEt/\hbar}\phi_{E,n}^{\pm}(z)dE \tag{7}$$

with arbitrary coefficients $c_n^{\pm}(E)$ and where $\phi_{E,n}^{\pm}(z)$ verify the time-independent Schrödinger equation

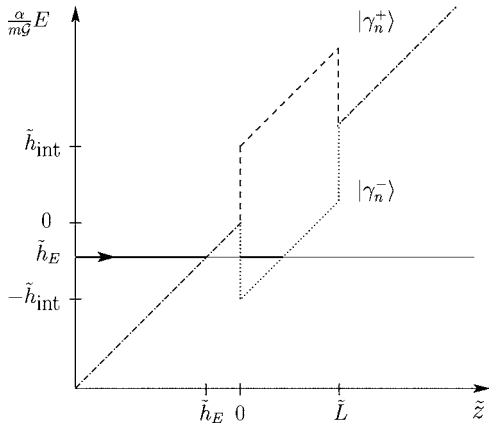

FIG. 3. Schematic representation of the energy E (solid line) of the atoms launched upwards upon a micromaser cavity of length L. The cavity containing n photons acts in the gravity linear field $m\mathcal{G}z$ as an additional repulsive potential (dashed) and an attractive one (dotted). The picture illustrates the case where the atom-field coupling is contant inside the cavity. Tilted symbols are dimensionless variables [see Eq. (9)].

$$\left(-\frac{\hbar^2}{2m}\frac{d^2}{dz^2} + m\mathcal{G}z + V_n^{\pm}(z)\right)\phi_{E,n}^{\pm}(z) = E\phi_{E,n}^{\pm}(z). \tag{8}$$

Introducing, for any length x, the dimensionless variable

$$\tilde{x} \equiv \alpha x \tag{9}$$

with

$$\alpha = \sqrt[3]{\frac{2m^2\mathcal{G}}{\hbar^2}}, \tag{10}$$

Eq. (8) reads

$$\left(-\frac{d^2}{d\tilde{z}^2} + \tilde{z} - \tilde{h}_E \pm \tilde{h}_{\rm int}u(\tilde{z})\right)\phi_{E,n}^{\pm}(\tilde{z}) = 0, \tag{11}$$

where

$$h_{\rm int} = h_g\sqrt{n+1}, \tag{12}$$

and

$$h_g = \frac{\hbar g}{m\mathcal{G}}. \tag{13}$$

For rubidium atoms, the characteristic length α^{-1} equals 0.3 μm and, roughly, the dimensionless variable $\tilde{h}_g$ is numerically equal to the interaction coupling strength $g/2\pi$ expressed in kHz. Similarly $\tilde{h}_E$ and $\tilde{L}$ yield the classical height h_E and the cavity length L, respectively, in thirds of μm.

Outside the cavity where the mode function vanishes (or can be considered as such), the wave functions satisfying Eq. (11) are linear combinations of Airy Ai and Bi functions [19] and $\phi_{E,n}^{\pm}(z)$ may be strictly generally written

$$\phi_{E,n}^{\pm}(z) = N_{E,n}^{\pm} \times \begin{cases} \mathrm{Ai}(\tilde{z} - \tilde{h}_E) \\ \quad \text{above the cavity}, \\ a_{E,n}^{\pm}\mathrm{Ai}(\tilde{z} - \tilde{h}_E) + b_{E,n}^{\pm}\mathrm{Bi}(\tilde{z} - \tilde{h}_E) \\ \quad \text{below the cavity}, \end{cases} \tag{14}$$

where $a_{E,n}^{\pm}$ and $b_{E,n}^{\pm}$ are two real coefficients unambiguously determined from the continuity conditions of the wave function and its first derivative at the lower cavity interface [where the coupling mode function $u(z)$ starts to be not null]. $N_{E,n}^{\pm}$ is a normalization constant that ensures

$$\int_{-\infty}^{+\infty} \phi_{E,n}^{\pm *}(z)\phi_{E',n}^{\pm}(z)dz = \delta(E - E'). \tag{15}$$

Using the normalization procedure for the wave functions belonging to a continuum spectrum [20], we get straightforwardly

$$N_{E,n}^{\pm} = \frac{N}{\sqrt{{a_{E,n}^{\pm}}^2 + {b_{E,n}^{\pm}}^2}}, \tag{16}$$

with $N = \sqrt{2m/\alpha\hbar^2}$.

In Eq. (14), the Airy Bi function does not appear above the cavity as it diverges for $z \to +\infty$. It is interesting to write the wave function (14) in the form

$$\phi_{E,n}^{\pm}(z) = N \times \begin{cases} \rho_{E,n}^{\pm -1}\mathrm{Ai}(\tilde{z} - \tilde{h}_E) \\ \quad \text{above the cavity}, \\ e^{-i\theta_{E,n}^{\pm}}\dfrac{\mathrm{Ai}(\tilde{z} - \tilde{h}_E) + i\,\mathrm{Bi}(\tilde{z} - \tilde{h}_E)}{2} \\ \quad + e^{i\theta_{E,n}^{\pm}}\dfrac{\mathrm{Ai}(\tilde{z} - \tilde{h}_E) - i\,\mathrm{Bi}(\tilde{z} - \tilde{h}_E)}{2} \\ \quad \text{below the cavity}, \end{cases} \tag{17}$$

where

$$\rho_{E,n}^{\pm} e^{i\theta_{E,n}^{\pm}} \equiv a_{E,n}^{\pm} + ib_{E,n}^{\pm}. \tag{18}$$

Equation (17) underlines that the wave functions $\phi_{E,n}^{\pm}(z)$ below the cavity consist of an upward and a downward wave (Ai$+i$ Bi and Ai$-i$ Bi, respectively). Indeed, the probability current densities $j = (i\hbar/2m)[\phi(d/dz)\phi^* - \phi^*(d/dz)\phi]$ associated to these two waves are respectively given by

$$j = \pm \frac{\alpha\hbar}{\pi m}. \tag{19}$$

For large negative $\tilde{z} - \tilde{h}_E$ values, these two waves behave similarly to plane waves with a z dependent wave vector. We have in this region [19]

$$\mathrm{Ai}(\tilde{z} - \tilde{h}_E) \pm i\,\mathrm{Bi}(\tilde{z} - \tilde{h}_E) \simeq \frac{e^{\pm i\pi/4}}{\sqrt{\pi}} \frac{e^{\pm ik(\tilde{z})(\tilde{z} - \tilde{h}_E)}}{(\tilde{h}_E - \tilde{z})^{1/4}}, \tag{20}$$

with $k(\tilde{z}) = 2/3(\tilde{h}_E - \tilde{z})^{1/2}$.

III. INDUCED EMISSION PROBABILITY

Let us assume that the atom is initially prepared in the excited state $|a\rangle$ and the cavity contains n photons. The center-of-mass motion is described by the initial wave packet $\phi(z)$. We denote by $\mathcal{A}^{\pm}(\tilde{h}_E)$ the coefficients of the development of $\phi(z)$ over the two bases $\{\phi_{E,n}^{\pm}(z)\}$:

$$\phi(z) = \int d\tilde{h}_E \mathcal{A}^{\pm}(\tilde{h}_E)\phi_{E,n}^{\pm}(z). \tag{21}$$

We thus consider the initial state of the system

$$|\psi(0)\rangle = \int dz\ \phi(z)|z,a,n\rangle \tag{22}$$

or more explicitly

$$\langle z|\psi(0)\rangle = \frac{1}{\sqrt{2}} \int d\tilde{h}_E [\mathcal{A}^{+}(\tilde{h}_E)\phi_{E,n}^{+}(z)|\gamma_n^{+}\rangle + \mathcal{A}^{-}(\tilde{h}_E)\phi_{E,n}^{-}(z)|\gamma_n^{-}\rangle]. \tag{23}$$

According to Eq. (7), the state of the system at any later time t is given by

$$\langle z|\psi(t)\rangle = \frac{1}{\sqrt{2}} \int d\tilde{h}_E e^{-i(\tilde{h}_E/\tilde{h}_g)gt} [\mathcal{A}^{+}(\tilde{h}_E)\phi_{E,n}^{+}(z)|\gamma_n^{+}\rangle + \mathcal{A}^{-}(\tilde{h}_E)\phi_{E,n}^{-}(z)|\gamma_n^{-}\rangle], \tag{24}$$

that is

$$\langle z|\psi(t)\rangle = \int d\tilde{h}_E e^{-i(\tilde{h}_E/\tilde{h}_g)gt} \times \left[\frac{1}{2}(\mathcal{A}^{+}(\tilde{h}_E)\phi_{E,n}^{+}(z) + \mathcal{A}^{-}(\tilde{h}_E)\phi_{E,n}^{-}(z))|a,n\rangle + \frac{1}{2}(\mathcal{A}^{+}(\tilde{h}_E)\phi_{E,n}^{+}(z) - \mathcal{A}^{-}(\tilde{h}_E)\phi_{E,n}^{-}(z))|b,n+1\rangle\right]. \tag{25}$$

A long time after the atom interacted with the cavity, according to Eq. (20), packets of the wave functions $\phi_{E,n}^{\pm}(z)$ reduce to packets of the sole downward wave components Ai$-i$ Bi below the cavity and we obtain

$$\langle z|\psi(t)\rangle = N \int d\tilde{h}_E e^{-i(\tilde{h}_E/\tilde{h}_g)gt} \times \left[\frac{1}{2}(\mathcal{A}^{+}(\tilde{h}_E)e^{i\theta_{E,n}^{+}} + \mathcal{A}^{-}(\tilde{h}_E)e^{i\theta_{E,n}^{-}})|a,n\rangle + \frac{1}{2}(\mathcal{A}^{+}(\tilde{h}_E)e^{i\theta_{E,n}^{+}} - \mathcal{A}^{-}(\tilde{h}_E)e^{i\theta_{E,n}^{-}})|b,n+1\rangle\right] \times \frac{\mathrm{Ai}(\tilde{z} - \tilde{h}_E) - i\,\mathrm{Bi}(\tilde{z} - \tilde{h}_E)}{2}\theta(-\tilde{z}), \tag{26}$$

where $\theta(\tilde{z})$ stands for the Heaviside step function.

It follows that the induced emission probability of a photon inside the cavity containing initially n photons is given,

at the end of the atom-cavity interaction, by

$$\mathcal{P}_{\mathrm{em}}(n) = \frac{1}{4}\int d\tilde{h}_E |\mathcal{A}^+(\tilde{h}_E)e^{i\theta^+_{E,n}} - \mathcal{A}^-(\tilde{h}_E)e^{i\theta^-_{E,n}}|^2. \quad (27)$$

Two limiting cases are particularly relevant from an experimental point of view [9–16]: the atom is launched from below upwards to the cavity, or the atom is simply dropped from above the cavity and passes down through it.

When the atom is launched upwards to the cavity and is initially described by the wave packet

$$\phi(z) = N\int d\tilde{h}_E \mathcal{A}(\tilde{h}_E)\frac{\mathrm{Ai}(\tilde{z}-\tilde{h}_E) + i\,\mathrm{Bi}(\tilde{z}-\tilde{h}_E)}{2}\theta(-\tilde{z}), \quad (28)$$

we may write

$$\phi(z) \simeq \int d\tilde{h}_E \mathcal{A}(\tilde{h}_E)e^{i\theta^\pm_{E,n}}\phi^\pm_{E,n}(z), \quad (29)$$

provided the atom is launched from sufficiently below the cavity [this is not a limiting condition as it is always possible from any starting point to tune the atomic energy components to any desired classical height h_E, giving rise to a turning point anywhere below ($h_E<0$), inside ($0<h_E<L$) or above the cavity region ($h_E>L$)]. Indeed, in this case, only packets of the upward wave components $\mathrm{Ai}+i\,\mathrm{Bi}$ contribute initially to the packets of the wave functions $\phi^\pm_{E,n}(z)$ [see Eq. (20)].

We thus have according to Eq. (21)

$$\mathcal{A}^\pm(\tilde{h}_E) \simeq \mathcal{A}(\tilde{h}_E)e^{i\theta^\pm_{E,n}}, \quad (30)$$

and the induced emission probability (27) simplifies to

$$\mathcal{P}_{\mathrm{em}}(n) = \int d\tilde{h}_E |\mathcal{A}(\tilde{h}_E)|^2 \sin^2(\theta^+_{E,n} - \theta^-_{E,n}). \quad (31)$$

As $|\mathcal{A}(\tilde{h}_E)|^2$ is the probability density of finding initially the atom in the monoenergetic state

$$\phi_{E,n}(z) = N\frac{\mathrm{Ai}(\tilde{z}-\tilde{h}_E) + i\,\mathrm{Bi}(\tilde{z}-\tilde{h}_E)}{2}, \quad (32)$$

we may interpret the coefficient

$$\mathcal{P}^\uparrow_{\mathrm{em}}(E,n) \equiv \sin^2(\theta^+_{E,n} - \theta^-_{E,n}) \quad (33)$$

in Eq. (31) as being the induced emission probability of a photon inside the cavity containing initially n photons by a monoenergetic atom of energy E launched upwardly in the excited state $|a\rangle$. Equation (33) is relevant for any value of the atomic energy E.

When the atom is dropped from above the cavity and is initially described by the free fall wave packet

$$\phi(z) = N\int d\tilde{h}_E \mathcal{A}(\tilde{h}_E)\mathrm{Ai}(\tilde{z}-\tilde{h}_E), \quad (34)$$

we may write

$$\phi(z) \simeq \int d\tilde{h}_E \mathcal{A}(\tilde{h}_E)\rho^\pm_{E,n}\phi^\pm_{E,n}(z), \quad (35)$$

provided the atom is released from *far* above the cavity ($h_E - L \gg h_{\mathrm{int}}$). Otherwise it is straightforward to check (e.g., numerically) that packets of $\rho^\pm_{E,n}\phi^\pm_{E,n}(z)$ diverge significantly inside and below the cavity compared to the same packets of pure $\mathrm{Ai}(\tilde{z}-\tilde{h}_E)$ functions that remain localized just above the cavity. These divergences get smeared as the initial wave packet increases its height above the cavity.

It then follows according to Eq. (21)

$$\mathcal{A}^\pm(\tilde{h}_E) \simeq \mathcal{A}(\tilde{h}_E)\rho^\pm_{E,n}, \quad (36)$$

and the induced emission probability (27) simplifies to

$$\mathcal{P}_{\mathrm{em}}(n) = \int d\tilde{h}_E |\mathcal{A}(\tilde{h}_E)|^2 \frac{1}{4}|\rho^+_{E,n}e^{i\theta^+_{E,n}} - \rho^-_{E,n}e^{i\theta^-_{E,n}}|^2. \quad (37)$$

Similarly to Eq. (33), we may interpret the coefficient

$$\mathcal{P}^\downarrow_{\mathrm{em}}(E,n) \equiv \frac{1}{4}|\rho^+_{E,n}e^{i\theta^+_{E,n}} - \rho^-_{E,n}e^{i\theta^-_{E,n}}|^2 \quad (38)$$

as being the induced emission probability of a photon inside the cavity containing initially n photons by a monoenergetic atom of energy E dropped from *far* above the cavity in the excited state $|a\rangle$. For atoms released *just* above the cavity, Eqs. (35)–(37) do not hold and no factor can be regarded as an induced emission probability of a monoenergetic excited atom. $\mathcal{P}_{\mathrm{em}}(n)$ must be computed using the general relation (27). Equation (38) is therefore only relevant for values of the atomic energy E such as h_E lies well above the cavity ($h_E - L \gg h_{\mathrm{int}}$).

It is important to note that an atom initially in the excited state $|a\rangle$ and launched upwards from below the cavity will be found at any later time in a linear combination of the $|a\rangle$ and $|b\rangle$ states according to Eq. (25). If the classical turning point is located just above the cavity, the wave packets of these two electronic states are never found completely located in this region and extend significantly inside the cavity. Hence an atom initially in the excited state $|a\rangle$ located just above the cavity cannot be seen like an intermediate state of an atom launched from the bottom in this electronic state. This explains why the treatments of both cases have not to be similar. More precisely, an atom initially in the excited state $|a\rangle$ located just above the cavity will be found to be an intermediate state of an atom launched from the bottom in a linear combination of the two electronic states with wave packets specific to each of these states. Such a case should be treated by a relation similar to Eq. (27), though generalized to any initial electronic state [as this equation only holds for atoms initially in the $|a\rangle$ state, see Eq. (22)].

In the special case where the atom-field coupling inside the cavity is constant along the atom propagation axis (mesa mode case: $u(z)=1$ inside the cavity, 0 elsewhere), the numbers $\rho^\pm_{E,n}$ and $\theta^\pm_{E,n}$ can be calculated analytically and this yields an explicit expression for the induced emission probabilities $\mathcal{P}^\uparrow_{\mathrm{em}}(E,n)$ and $\mathcal{P}^\downarrow_{\mathrm{em}}(E,n)$. Inside the cavity, the stationary wave functions (14) read

$$\phi^{\pm}_{E,n}(z) = N^{\pm}_{E,n}(p^{\pm}_{E,n}\mathrm{Ai}(\tilde{z}-\tilde{h}_E \pm \tilde{h}_{\mathrm{int}}) + q^{\pm}_{E,n}\mathrm{Bi}(\tilde{z}-\tilde{h}_E \pm \tilde{h}_{\mathrm{int}})) \tag{39}$$

and the continuity conditions at the cavity interfaces yield

$$p^{\pm}_{E,n} = \pi W^{\pm}_{ab}(-\tilde{h}_E + \tilde{L}), \tag{40}$$

$$q^{\pm}_{E,n} = -\pi W^{\pm}_{aa}(-\tilde{h}_E + \tilde{L}), \tag{41}$$

$$a^{\pm}_{E,n} = \pi^2 \begin{vmatrix} W^{\pm}_{aa}(-\tilde{h}_E + \tilde{L}) & W^{\pm}_{ab}(-\tilde{h}_E + \tilde{L}) \\ W^{\pm}_{ba}(-\tilde{h}_E) & W^{\pm}_{bb}(-\tilde{h}_E) \end{vmatrix}, \tag{42}$$

$$b^{\pm}_{E,n} = \pi^2 \begin{vmatrix} W^{\pm}_{aa}(-\tilde{h}_E) & W^{\pm}_{ab}(-\tilde{h}_E) \\ W^{\pm}_{aa}(-\tilde{h}_E + \tilde{L}) & W^{\pm}_{ab}(-\tilde{h}_E + \tilde{L}) \end{vmatrix}, \tag{43}$$

with

$$W^{\pm}_{aa}(\tilde{z}) = W(\mathrm{Ai}(\tilde{z}), \mathrm{Ai}(\tilde{z} \pm \tilde{h}_{\mathrm{int}})), \tag{44}$$

$$W^{\pm}_{ab}(\tilde{z}) = W(\mathrm{Ai}(\tilde{z}), \mathrm{Bi}(\tilde{z} \pm \tilde{h}_{\mathrm{int}})), \tag{45}$$

$$W^{\pm}_{ba}(\tilde{z}) = W(\mathrm{Bi}(\tilde{z}), \mathrm{Ai}(\tilde{z} \pm \tilde{h}_{\mathrm{int}})), \tag{46}$$

$$W^{\pm}_{bb}(\tilde{z}) = W(\mathrm{Bi}(\tilde{z}), \mathrm{Bi}(\tilde{z} \pm \tilde{h}_{\mathrm{int}})), \tag{47}$$

where W designates the Wronskian:

$$W(f(z), g(z)) \equiv \begin{vmatrix} f(z) & g(z) \\ f'(z) & g'(z) \end{vmatrix}, \quad \forall f(z), g(z). \tag{48}$$

Similarly to the approach used in the description of the cold atom micromaser in the horizontal configuration [1,2], we focus hereafter on the properties of the induced emission probabilities of a monoenergetic beam [here $\mathcal{P}^{\uparrow}_{\mathrm{em}}(E,n)$ and $\mathcal{P}^{\downarrow}_{\mathrm{em}}(E,n)$] without particularization to any atomic spatial structure. $\mathcal{P}^{\uparrow}_{\mathrm{em}}(E,n)$ is studied depending on whether the atomic kinetic energy (or the lack of this energy) at the cavity interfaces is much higher than the interaction energy ($|h_E| \gg h_{\mathrm{int}}$ and $|h_E - L| \gg h_{\mathrm{int}}$) or much lower. We call each case the hot and cold atom regime, respectively. $\mathcal{P}^{\downarrow}_{\mathrm{em}}(E,n)$ being only relevant for $|h_E - L| \gg h_{\mathrm{int}}$, it is described in the sole hot atom regime section and is not concerned with the cold atom regime.

A. Hot atom regime: Rabi limit

In the hot atom regime, the arguments $-\tilde{h}_E$ and $-\tilde{h}_E + \tilde{L}$ in Eqs. (40)–(43) are in absolute value much larger than $\tilde{h}_{\mathrm{int}}$. For such large arguments, simplified expressions of the Wronskians (44)–(47) can be obtained using the asymptotic expansions of the Airy functions [19]. We have for $|\tilde{z}| \gg \tilde{h}_{\mathrm{int}}$, $|\tilde{z}| \gg 1$

$$W^{\pm}_{aa}(-\tilde{z}) \simeq \mp \frac{1}{\pi} \sin(\tilde{h}_{\mathrm{int}} \tilde{z}^{1/2}), \tag{49}$$

$$W^{\pm}_{ab}(-\tilde{z}) \simeq \frac{1}{\pi} \cos(\tilde{h}_{\mathrm{int}} \tilde{z}^{1/2}), \tag{50}$$

$$W^{\pm}_{ba}(-\tilde{z}) \simeq -\frac{1}{\pi} \cos(\tilde{h}_{\mathrm{int}} \tilde{z}^{1/2}), \tag{51}$$

$$W^{\pm}_{bb}(-\tilde{z}) \simeq \mp \frac{1}{\pi} \sin(\tilde{h}_{\mathrm{int}} \tilde{z}^{1/2}), \tag{52}$$

$$W^{\pm}_{aa}(\tilde{z}) \simeq \mp \frac{1}{8\pi} \frac{\tilde{h}_{\mathrm{int}}}{\tilde{z}} e^{-(4/3)\tilde{z}^{3/2}}, \tag{53}$$

$$W^{\pm}_{ab}(\tilde{z}) \simeq \frac{1}{\pi} e^{\pm \tilde{h}_{\mathrm{int}} \tilde{z}^{1/2}}, \tag{54}$$

$$W^{\pm}_{ba}(\tilde{z}) \simeq -\frac{1}{\pi} e^{\mp \tilde{h}_{\mathrm{int}} \tilde{z}^{1/2}}, \tag{55}$$

$$W^{\pm}_{bb}(\tilde{z}) \simeq \pm \frac{1}{2\pi} \frac{\tilde{h}_{\mathrm{int}}}{\tilde{z}} e^{(4/3)\tilde{z}^{3/2}}. \tag{56}$$

We then find straightforwardly $\rho^{\pm}_{E,n} \simeq 1$ for $\tilde{h}_E > \tilde{L}$,

$$\theta^{\pm}_{E,n} \simeq \begin{cases} \mp \tilde{h}_{\mathrm{int}}(\sqrt{\tilde{h}_E} - \sqrt{\tilde{h}_E - \tilde{L}}) & \text{if } \tilde{h}_E > \tilde{L}, \\ \mp \tilde{h}_{\mathrm{int}} \sqrt{\tilde{h}_E} & \text{if } 0 < \tilde{h}_E < \tilde{L}, \\ \pi & \text{if } \tilde{h}_E < 0, \end{cases} \tag{57}$$

and thus, from Eqs. (33) and (38),

$$\mathcal{P}^{\uparrow}_{\mathrm{em}}(E,n) \simeq \begin{cases} \sin^2(2\tilde{h}_{\mathrm{int}}[\sqrt{\tilde{h}_E} - \sqrt{\tilde{h}_E - \tilde{L}}]) & \text{if } \tilde{h}_E > \tilde{L}, \\ \sin^2(2\tilde{h}_{\mathrm{int}} \sqrt{\tilde{h}_E}) & \text{if } 0 < \tilde{h}_E < \tilde{L}, \\ 0 & \text{if } \tilde{h}_E < 0, \end{cases} \tag{58}$$

and, for $\tilde{h}_E > \tilde{L}$,

$$\mathcal{P}^{\downarrow}_{\mathrm{em}}(E,n) \simeq \sin^2(\tilde{h}_{\mathrm{int}}[\sqrt{\tilde{h}_E} - \sqrt{\tilde{h}_E - \tilde{L}}]). \tag{59}$$

Equations (58) and (59) are nothing else than the well known Rabi formula

$$\mathcal{P}_{\mathrm{em}}(E,n) = \sin^2\left(\frac{\Omega_n \tau}{2}\right), \tag{60}$$

where $\Omega_n = 2g\sqrt{n+1}$ and τ is the classical transit time of an atom of energy E through the cavity. For $\tilde{h}_E < 0$, the atom launched upwards does not reach the cavity and no induced emission process occurs (the classical interaction time τ is null). For $0 < \tilde{h}_E < \tilde{L}$, the atom turns back inside the cavity and the interaction time does not depend on the cavity length L. For $\tilde{h}_E > \tilde{L}$, the atom launched upwards passes twice inside the cavity (upwards and downwards) and the interaction time is L dependent, while the atom dropped from above passes only once with half the interaction time, all other conditions being equivalent.

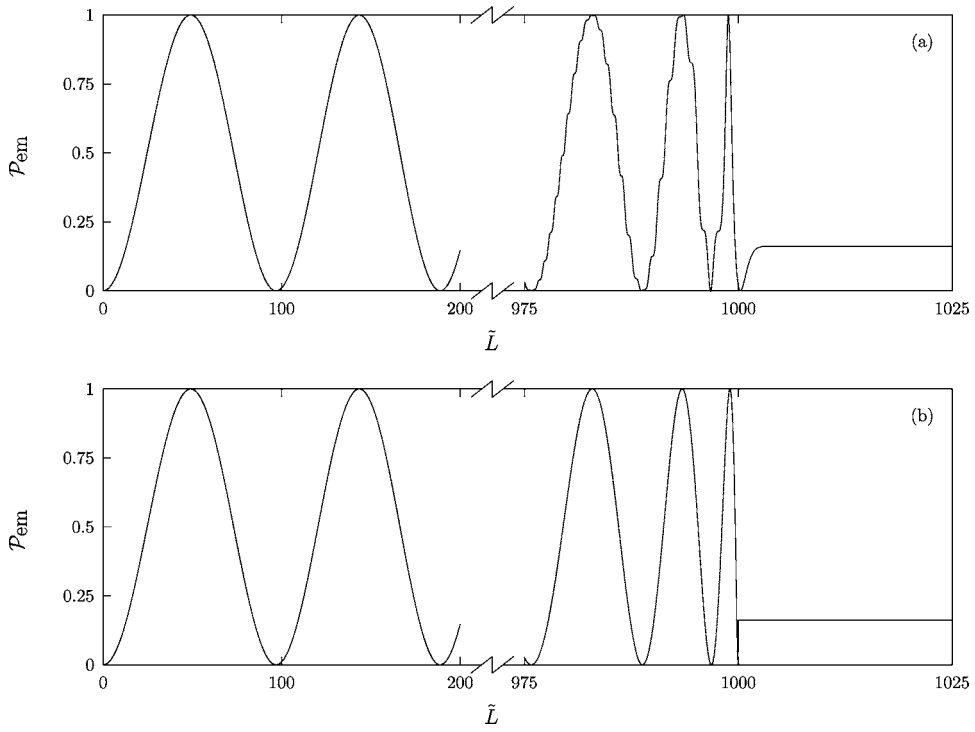

FIG. 4. Induced emission probability $\mathcal{P}_{\rm em}$ as a function of the cavity length with (a) and without (b) quantization of the atomic motion (hot atom regime: $\tilde{h}_E=1000$ and $\tilde{h}_{\rm int}=1$). Tilted variables are dimensionless [see Eq. (9)].

We illustrate in Figs. 4(a) and 4(b) the induced emission probability $\mathcal{P}_{\rm em}\equiv\mathcal{P}_{\rm em}^{\uparrow}(E,n)$ as a function of the cavity length for $\tilde{h}_E\gg\tilde{h}_{\rm int}$, respectively with and without quantization of the atomic motion [Eqs. (33) and (58), respectively]. We well observe that both results are in accordance, except in the region where $\tilde{L}\approx\tilde{h}_E$. In this region, $|\tilde{h}_E-\tilde{L}|$ is not much greater than $\tilde{h}_{\rm int}$ and we are out of the validity domain of the approximated expression (58). The small additional oscillations observed in the induced emission probability curve where $\tilde{L}\approx\tilde{h}_E$ are pure quantum effects originating from the quantization of the atomic motion. These effects arise when the cavity length matches nearly the classical turning point of the atom in the gravitational field. In this case, the potential barrier and well $V_n^{\pm}(z)$ play a significant role as the kinetic energy of the atoms is very small exactly where the potential energy exhibits strong variations.

B. Cold atom regime

1. Negative energy resonances

In the cold atom regime, the induced emission probability $\mathcal{P}_{\rm em}$ exhibits a completely different behavior. This is first illustrated in Figs. 5 and 6 that show $\mathcal{P}_{\rm em}$ as a function of the total atomic energy and the cavity length, respectively. In contrast to the hot atom regime governed by a sine behavior of $\mathcal{P}_{\rm em}$, fine resonances are presently observed, even in the negative energy domain [$E<0$, i.e., $h_E<0$, see Eq. (2)] where classically the atom does not reach the cavity and cannot therefore emit any photon in there. This pure quantum effect arises from resonant diffusion processes over quasibound states of the potential $V_n^{-}(z)$. Quasibound states are those states related to unbound potentials containing a local minimum [like $V_n^{-}(z)$, see Fig. 3]. A particle initially confined in the potential well may remain there for an extremely long time, before escaping by tunnel effect to the lower potential

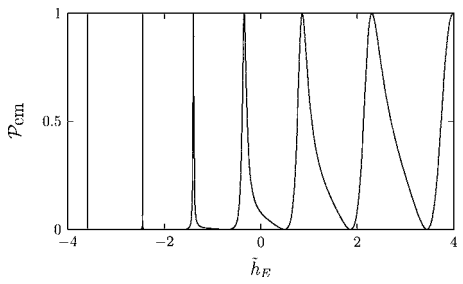

FIG. 5. Induced emission probability $\mathcal{P}_{\rm em}$ with respect to the particle energy for $\tilde{L}=10$ and $\tilde{h}_{\rm int}=10$.

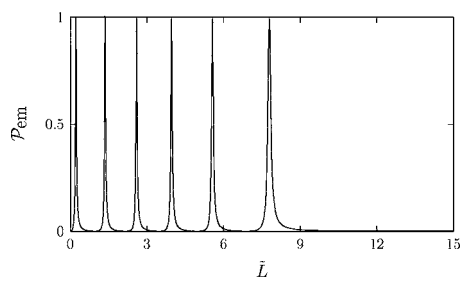

FIG. 6. Induced emission probability $\mathcal{P}_{\rm em}$ with respect to the cavity length for $\tilde{h}_E=-1$ and $\tilde{h}_{\rm int}=10$.

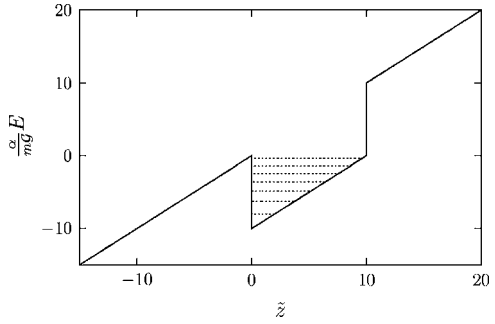

FIG. 7. $V_n^-(z)$ quasibound state energy levels for $\tilde{L}=10$ and $\tilde{h}_{\rm int}=10$.

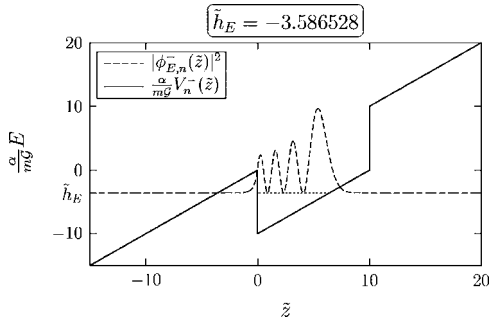

FIG. 8. Stationary probability density $|\phi^-_{E,n}(z)|^2$ (in a.u.) for E matching a quasibound state energy of the potential $V_n^-(z)$ ($\tilde{L}=10$ and $\tilde{h}_{\rm int}=10$).

region. These states are easily found by looking for the solutions of the stationary Schrödinger equation that represent a pure outgoing wave for $z\to-\infty$ [20,21]. In the case of a mesa mode function, these solutions are given by

$$\phi^{-,\mathrm{out}}_{E,n}(z) = N'^-_{E,n} \times \begin{cases} \mathrm{Ai}(\tilde{z}-\tilde{h}_E) \\ \quad \text{if } z > L, \\ v'^-_{E,n}\mathrm{Ai}(\tilde{z}-\tilde{h}_E-\tilde{h}_{\rm int}) + w'^-_{E,n}\mathrm{Bi}(\tilde{z}-\tilde{h}_E-\tilde{h}_{\rm int}) \\ \quad \text{if } 0 < z < L, \\ d'^-_{E,n}(\mathrm{Ai}(\tilde{z}-\tilde{h}_E) - i\,\mathrm{Bi}(\tilde{z}-\tilde{h}_E)) \\ \quad \text{if } z < 0. \end{cases} \tag{61}$$

The continuity conditions of the wave function and its derivative at the cavity interfaces yield an homogenous system of equations for the coefficients $N'^-_{E,n}$, $v'^-_{E,n}$, $w'^-_{E,n}$ and $d'^-_{E,n}$.

Non trivial solutions of this system do only exist for a well defined set of complex values of E. Writing these values

$$E = E_0 - i\frac{\Gamma}{2}, \tag{62}$$

E_0 and $\hbar\Gamma^{-1}$ yield the energy and the characteristic escape time of the quasibound states.

We illustrate in Fig. 7 the $V_n^-(z)$ quasibound states for the cavity parameters considered in Fig. 5. The values of $\tilde{h}_{E_0}$ and $\tilde{h}_\Gamma$ for these quasibound states are given in Table I. We well notice that the energies of these states correspond exactly to the particle energies for which a narrow resonance in the induced emission probability is observed (Fig. 5). Γ yields the resonance peak width.

TABLE I. Negative energy quasibound state $\tilde{h}_{E_0}$ and $\tilde{h}_\Gamma$ values for $\tilde{L}=10$ and $\tilde{h}_{\rm int}=10$.

$\tilde{h}_{E_0}$	$\tilde{h}_\Gamma$
−0.35	1.0×10^{-1}
−1.397	2.3×10^{-2}
−2.4504	1.8×10^{-3}
−3.586528	4.3×10^{-5}
−4.83661911	3.0×10^{-7}
−6.25546372124	4.3×10^{-10}
−7.992076463882778	4.6×10^{-14}

At a fixed total atomic energy E, the quasibound state energies vary with the cavity length. Whenever such a state energy matches the atomic E value, the induced emission probability is optimized and a resonance in the curve of $\mathcal{P}_{\rm em}$ with respect to the cavity length is observed (Fig. 6). In this sense, the physical interpretation of the resonances in the induced emission probability differs significantly from what happens with the micromaser in a horizontal configuration where the effects of the gravitation on the quantum atomic motion are not taken into account [1,2]. Also, it is interesting to note that the resonance amplitudes for the micromaser in the vertical configuration reaches 1 whereas they are limited to 0.5 in the horizontal configuration.

More physically, the behavior of the stationary wave function $\phi^-_{E,n}(z)$ [Eqs. (17) and (39)] differs significantly depending on whether the particle energy E corresponds to a quasibound state energy or not. This is illustrated in Figs. 8 and 9. In the first case, the particle is launched upwards to the cavity with a total energy matching a quasibound state energy of the potential $V_n^-(z)$. The stationary wave function $\phi^-_{E,n}(z)$ enters significantly inside the cavity by tunnel effect. Consequently, a strong interaction between the atom and the cavity

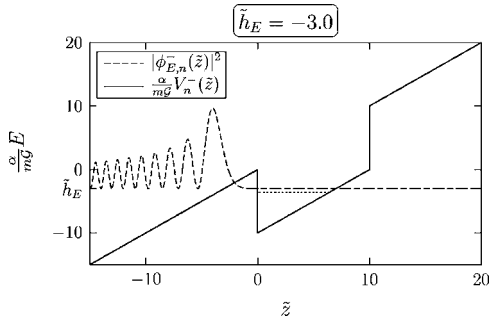

FIG. 9. Stationary probability density $|\phi^-_{E,n}(z)|^2$ (in a.u.) for E different than the quasibound state energies of the potential $V_n^-(z)$ ($\tilde{L}=10$ and $\tilde{h}_{\rm int}=10$).

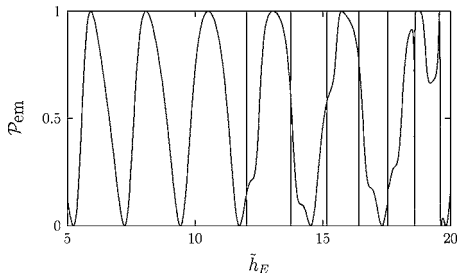

FIG. 10. Induced emission probability $\mathcal{P}_{em}$ with respect to the particle energy for $\tilde{L}=10$ and $\tilde{h}_{int}=10$.

field may occur and the induced emission probability is found to be equal to 1. When considering a realistic atomic wave packet, this effect is of course restricted to the components $\mathcal{A}(\tilde{h}_E)$ of the wave packet for which $\tilde{h}_E$ falls within the width $\tilde{h}_\Gamma$ of the quasibound state. Inversely, if the particle energy does not match a quasibound state energy (Fig. 9), the stationary wave function does not enter into the cavity and no atom-field interaction can take place. In this case, the induced emission probability drops down to zero.

In any case, the wave function $\phi^+_{E,n}(z)$ is reflected at the classical turning point for any negative value of the total energy [like $\phi^-_{E,n}(z)$ in Fig. 9] and never contributes to the induced emission process for these energy values as it does not enter inside the cavity.

2. Positive energy resonances

Fine resonances for positive values of the particle energy ($E>0$, i.e., $h_E>0$) are also observed. This is illustrated in Fig. 10 that shows the induced emission probability as a function of the total atomic energy. In the positive energy domain, fine resonances occur for $h_E>L$ and they arise from resonant diffusion processes over quasibound states of the potential $V^+_n(z)$ (see Fig. 11). In the vicinity of such a quasibound state, the $\phi^+_{E,n}(z)$ wave function overcomes the $V^+_n(z)$ potential barrier and extends beyond the top of the cavity, whereas this wave function is usually restricted below the potential barrier for ordinary values of E. This significant change in the behavior of the $\phi^+_{E,n}(z)$ wave function near the $V^+_n(z)$ quasibound states affects strongly the interplay between this wave function and the $\phi^-_{E,n}(z)$ one, which always extends beyond the top of the cavity for any value of E in

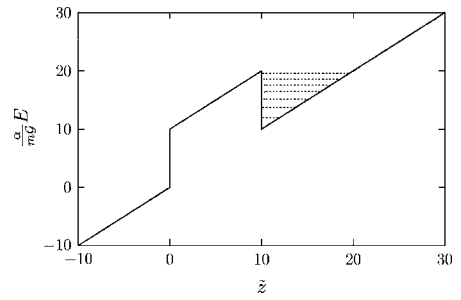

FIG. 11. $V^+_n(z)$ quasibound state energy levels for $\tilde{L}=10$ and $\tilde{h}_{int}=10$.

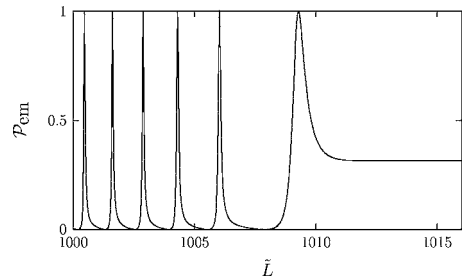

FIG. 12. Induced emission probability $\mathcal{P}_{em}$ with respect to the cavity length for $\tilde{h}_E=8.5$ and $\tilde{h}_{int}=1000$.

this energy domain. Therefore and in constrast to the $a^-_{E,n}$ and $b^-_{E,n}$ coefficients of the $\phi^-_{E,n}(z)$ wave function [see Eq. (14)] that vary smoothly with E, the $a^+_{E,n}$ and $b^+_{E,n}$ coefficients vary significantly around the $V^+_n(z)$ quasibound states, resulting in strong and rapid variations of the induced emission probability in these regions. These variations are found to occur between 0 and 1, corresponding to destructive and constructive interferences between the two wave functions $\phi^\pm_{E,n}(z)$, respectively.

3. Cavity length effects

In the hot atom regime and in the positive energy domain, the induced emission probability is independent of the cavity length L as soon as this length is greater than h_E [see Eq. (58)]. In the cold atom regime, this statement must be revised and holds only when $L \gtrsim h_E+h_{int}$. In this case indeed, the classical turning points where the $\phi^+_{E,n}(z)$ and $\phi^-_{E,n}(z)$ wave functions drop down to zero are given by $z=\max(h_E-h_{int},0)$ and $z=h_E+h_{int}$, respectively. Thus, any variation of the cavity length beyond $\sim(h_E+h_{int})$ does not affect anymore the spatial dependence of the wave functions and the induced emission probability becomes L independent. This is illustrated in Fig. 12 that shows the induced emission probability $\mathcal{P}_{em}$ with respect to the cavity length for $\tilde{h}_E=8.5$ and $\tilde{h}_{int}=1000$. $\mathcal{P}_{em}$ starts to be constant only beyond $\tilde{L}=\tilde{h}_E+\tilde{h}_{int}=1008.5$.

4. Sine and Gaussian mode functions

The fine resonances of the induced emission probability observed in the cold atom regime are not restricted to the case of the mesa mode investigated so far here. Using nu-

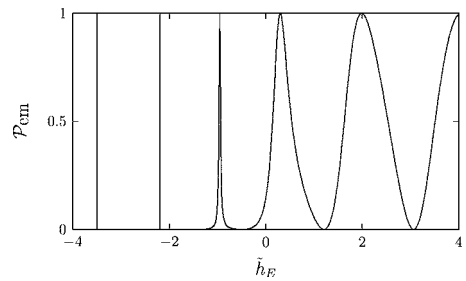

FIG. 13. Induced emission probability $\mathcal{P}_{em}$ with respect to the particle energy for $\tilde{L}=10$ and $\tilde{h}_{int}=10$, sine mode.

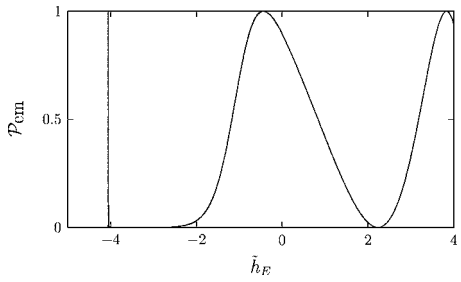

FIG. 14. Induced emission probability $\mathcal{P}_{\rm em}$ with respect to the particle energy for $\tilde{L}=10$ and $\tilde{h}_{\rm int}=10$, Gaussian mode.

merical procedures [22], we have computed the solutions $\phi^{\pm}_{E,n}(z)$ of the stationary Schrödinger equation (11) for sine and gaussian mode functions $[u(z)=\sin(\pi z/L)$ for $0<z<L$, 0 elsewhere and $u(z)=e^{-(z-L/2)^2/2\sigma^2}$ with $\sigma=\sqrt{2/\pi}L$, respectively]. We show in Figs. 13 and 14 the related induced emission probability $\mathcal{P}_{\rm em}$ with respect to the total atomic energy. The fine negative energy resonances observed in the curves arise from the same interaction of the atomic wave function with the quasibound states of the potential $V_n^-(z)$. Those are illustrated in Fig. 15 for the sine mode. As any mode function will give rise to such quasibound states (provided $\tilde{h}_{\rm int}$ is large enough), the resonances in the induced emission probability will be a very general feature of the vertical micromaser in the cold atom regime, in contrast to what happens with the horizontal micromaser where the induced emission probability characteristics are much more mode dependent [3]. This defines a very interesting property as it should help the experimenters to observe the particular behavior of the induced emission probability in the cold atom regime, whatever the exact mode function of the cavity. Positive and negative energy quasibound state resonances are an extremely robust feature of the mazer action in the vertical geometry.

C. Intermediate regime

We define the intermediate regime by $h_E \approx L+h_{\rm int}$. In this regime, when h_E starts to be greater than $L+h_{\rm int}$, the particle energy lies above the potentials $V_n^{\pm}(z)$ ($\tilde{h}_E>20$ in Fig. 11) and the effects of these potentials start to decrease all the more that the particle energy increases. In this case, the cold atom regime is left and we enter the hot atom one where the

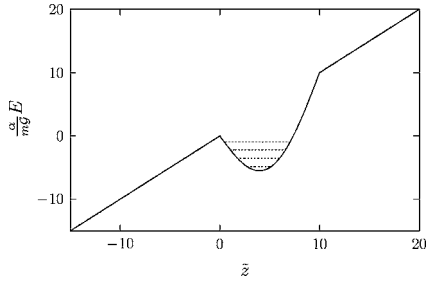

FIG. 15. $V_n^-(z)$ quasibound state energy levels for $\tilde{L}=10$ and $\tilde{h}_{\rm int}=10$, sine mode.

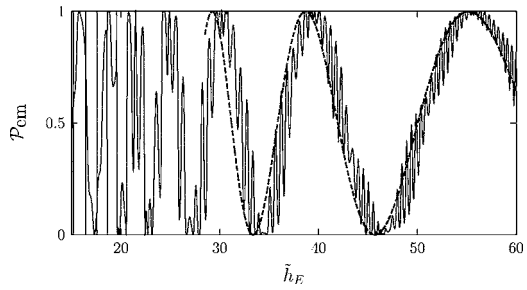

FIG. 16. Induced emission probability $\mathcal{P}_{\rm em}$ with respect to the particle energy for $\tilde{L}=10$ and $\tilde{h}_{\rm int}=10$, mesa mode [the dashed line represents the classical limit given by Eq. (58)].

classical results hold. This is illustrated in Fig. 16 which shows that for $h_E>L+h_{\rm int}$, the induced emission probability starts to oscillate more and more regularly between 0 and 1, reaching the classical oscillations as soon as the particle energy value is sufficiently high (Fig. 16 does not extend up to the classical limit where the additional small oscillations have smeared out).

IV. PHOTON STATISTICS

When the micromaser is pumped by a flux of excited atoms launched upwards and dissipation is considered, a steady-state photon number distribution $\mathcal{P}(n)$ is established inside the cavity. This distribution is given by [2]

$$\mathcal{P}(n)=\mathcal{P}(0)\prod_{m=1}^{n}\frac{Cn_b+r\mathcal{P}_{\rm em}(m-1)/m}{C(n_b+1)}, \tag{63}$$

where r is the atomic injection rate, C the cavity decay rate and n_b the number of photons inside the cavity in thermal equilibrium. In the cold atom regime, unusual "dragon" photon number distributions $\mathcal{P}(n)$ have been predicted by Meyer *et al.* [2]. For the vertical micromaser, Eq. (63) still holds provided Eq. (33) is used to compute the induced emission probability $\mathcal{P}_{\rm em}(n)$. We show in Fig. 17 the photon number distribution $\mathcal{P}(n)$ obtained in the mesa mode case for $r/C=10^4$, $n_b=20$, $\tilde{h}_g=\tilde{L}=100$ and $\tilde{h}_E=-2$. This figure illustrates that remarkably the unusual "dragon" distributions are preserved in the vertical configuration. This result is extremely interesting as it shows that a vertical micromaser in the cold regime (in principle experimentally more feasible) could be

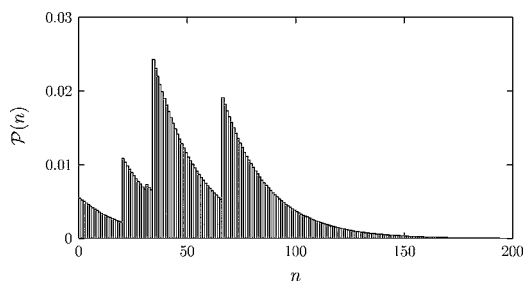

FIG. 17. Steady-state photon number distribution $\mathcal{P}(n)$ ($r/C=10^4$, $n_b=20$, $\tilde{h}_g=\tilde{L}=100$, and $\tilde{h}_E=-2$, mesa mode).

used rather than a horizontal one to demonstrate the highly nonclassical "dragon" photon number distributions [23]. It is also interesting to point out that this distribution is obtained for a flux of incident atoms classically not reaching the cavity. Similar distributions are obtained when considering other values of $\tilde{h}_E$, including positive ones. Each maximum in the dragon photon number distribution $\mathcal{P}(n)$ occurs at n values maximizing $\mathcal{P}_{\mathrm{em}}(n)$. The width of the resonances in the induced emission probability determines therefore the acceptable level of noise in the atomic kinetic energy that preserves the shape of the photon number distribution.

V. SUMMARY

In this paper we have presented the quantum theory of the cold atom micromaser in a vertical configuration, considering gravity action on the quantized atomic motion. Analytical expressions for the atom-field wave functions and the induced emission probability have been obtained in the special case of the constant cavity mode. Interesting effects related to the vertical geometry have been pointed out. In particular, we have shown that the cavity containing n photons acts in the gravity linear field as an additional repulsive and attractive potential, resulting in quasibound states of the atomic motion that enhance significantly the induced emission probability of a photon inside the cavity as soon as the total atomic energy matches one of these states. This feature give rise to fine resonances in the induced emission probability and is not restricted to any particular cavity mode function. This should make easier any experimental demonstration of these effects. We have also shown that an atom is able to emit a photon inside the cavity, though classically it does not reach the interaction region. This peculiarity is related to the cavity potential quasibound states that enable the particle to enter inside the cavity by tunnel effect. It has also been demonstrated that the classical results are well recovered for hot atoms where the quantization of the atomic motion is unnecessary. Finally, we have shown that the unusual "dragon" photon number distribution predicted when a horizontal micromaser is pumped by a flux of excited atoms might also be observed in the vertical geometry, even with a flux of atoms that classically do not reach the cavity.

ACKNOWLEDGMENTS

This work has been supported by the Belgian Institut Interuniversitaire des Sciences Nucléaires (IISN). J.M. thanks the Belgian FRIA for financial support.

[1] M. O. Scully, G. M. Meyer, and H. Walther, Phys. Rev. Lett. **76**, 4144 (1996).
[2] G. M. Meyer, M. O. Scully, and H. Walther, Phys. Rev. A **56**, 4142 (1997).
[3] M. Löffler, G. M. Meyer, M. Schröder, M. O. Scully, and H. Walther, Phys. Rev. A **56**, 4153 (1997).
[4] O. Benson, M. Weidinger, M. Löffler, and H. Walther, Fortschr. Phys. **46**, 809 (1998).
[5] T. Bastin and J. Martin, Phys. Rev. A **67**, 053804 (2003).
[6] T. E. I. Bloch and T. W. Hänsch, Nature (London) **403**, 166 (2000).
[7] V. V. Nesvizhevsky, H. G. Börner, A. K. Petoukhov, H. Abele, S. Baeler, F. J. Rue, T. Stöferle, A. Westphal, A. M. Gagarski, G. A. Petrov, *et al.*, Nature (London) **415**, 297 (2002).
[8] V. V. Nesvizhevsky, H. G. Börner, A. M. Gagarski, A. K. Petoukhov, G. A. Petrov, H. Abele, S. Baeler, G. Divkovic, F. J. Rue, T. Stöferle, *et al.*, Phys. Rev. D **67**, 102002 (2003).
[9] H. Mabuchi, Q. A. Turchette, M. S. Chapman, and J. Kimble, Opt. Lett. **21**, 1393 (1996).
[10] C. J. Hood, M. S. Chapman, T. W. Lynn, and H. J. Kimble, Phys. Rev. Lett. **80**, 4157 (1998).
[11] P. Münstermann, T. Fischer, P. Maunz, P. W. H. Pinkse, and G. Rempe, Phys. Rev. Lett. **82**, 3791 (1999).
[12] P. Münstermann, T. Fischer, P. Pinkse, and G. Rempe, Opt. Commun. **159**, 63 (1999).
[13] J. Ye, D. W. Vernooy, and H. J. Kimble, Phys. Rev. Lett. **83**, 4987 (1999).
[14] M. Hennrich, T. Legero, A. Kuhn, and G. Rempe, Phys. Rev. Lett. **85**, 4872 (2000).
[15] Y. Shimizu, N. Shiokawa, N. Yamamoto, M. Kozuma, T. Kuga, L. Deng, and E. W. Hagley, Phys. Rev. Lett. **89**, 233001 (2002).
[16] P. Maunz, T. Puppe, I. Schuster, N. Syassen, P. W. H. Pinkse, and G. Rempe, Nature (London) **428**, 50 (2004).
[17] K.-P. Marzlin and J. Audretsch, Phys. Rev. A **53**, 1004 (1996).
[18] Xu-Bo Zou and Jing-Bo Xu, Phys. Rev. A **61**, 063409 (2000).
[19] M. Abramowitz and I. Stegun, *Handbook of Mathematical Functions* (Dover Publications, New York, 1970).
[20] L. D. Landau and E. M. Lifshitz, *Quantum Mechanics-Non-Relativistic Theory*, 2nd ed. (Pergamon, London, 1965).
[21] D. Ahn and S. L. Chuang, Phys. Rev. B **34**, R9034 (1986).
[22] T. Bastin and E. Solano, Comput. Phys. Commun. **124**, 197 (2000).
[23] C. T. Lee, J. Opt. Soc. Am. B **14**, 1576 (1997).